10-2002

Fluctuations and bistability in a "hybrid" atomistic model for CO oxidation on nanofacets: An effective potential analysis

Da-Jiang Liu
Ames Laboratory, dajiang@fi.ameslab.gov

James W. Evans
Iowa State University, evans@ameslab.gov

Fluctuations and bistability in a "hybrid" atomistic model for CO oxidation on nanofacets: An effective potential analysis

Abstract
An analysis on the existence of bistability in the hybrid reaction model for CO oxidation in finite systems is demonstrated. As such, numerical evidence to indicate the existence of an effective potential characterizing this behavior is provided. This potential is determined by exact kinetic Monte Carlo (KMC) simulation analysis, but reasonable estimate available from approximate master equations, and from Fokker-Planck equations which are obtained from further approximation of the master equations.

Keywords
adsorption, computer simulation, desorption, diffusion, Monte Carlo methods, nucleation, order disorder transitions, oxidation, probability distributions, random processes, statistical mechanics, superlattices, atomistic model, fluctuation-induced transitions, Fokker-Planck equations, nanofacets, stochastic theories

Comments
The following article appeared in *Journal of Chemical Physics* 117, 15 (2002): 7319 and may be found at doi:10.1063/1.1507105.

Fluctuations and bistability in a "hybrid" atomistic model for CO oxidation on nanofacets: An effective potential analysis

Da-Jiang Liu and J. W. Evans

Citation: The Journal of Chemical Physics **117**, 7319 (2002); doi: 10.1063/1.1507105
View online: http://dx.doi.org/10.1063/1.1507105
View Table of Contents: http://scitation.aip.org/content/aip/journal/jcp/117/15?ver=pdfcov
Published by the AIP Publishing

Fluctuations and bistability in a "hybrid" atomistic model for CO oxidation on nanofacets: An effective potential analysis

Da-Jiang Liu[a] and J. W. Evans[b]
Ames Laboratory, USDOE, Iowa State University, Ames, Iowa 50011

(Received 12 April 2002; accepted 24 July 2002)

We analyze fluctuations in a "hybrid" atomistic model mimicking CO oxidation on nanoscale facets of metal(100) catalyst surfaces. The model incorporates a mean-field-like treatment of infinitely mobile CO, and a lattice-gas treatment of the superlattice ordering of immobile O. For an infinite system, it exhibits an Ising-type order–disorder transition for O, together with mean-field-like bistability disappearing at a cusp bifurcation. For finite systems, we use kinetic Monte Carlo simulation to study the probability distribution for the population of adsorbed species, from which bistability can be observed, together with fluctuation-induced transitions between the two stable states. An effective potential picture emerges from our analyses that can be used to quantify both the system size dependence of fluctuations and the transition rates. Thus, our hybrid atomistic model displays fluctuation behavior analogous to traditional mean-field models. This qualitative behavior can be understood by approximate treatments of population dynamics using master equations and Fokker–Planck equations. A generalized model with finite mobility of CO is also analyzed for comparison with the hybrid model. In contrast, it exhibits fluctuation behavior akin to equilibrium systems with Ising-type first-order transitions. © *2002 American Institute of Physics.*
[DOI: 10.1063/1.1507105]

I. INTRODUCTION

The study of fluctuations in a variety of (finite) physical and chemical systems provides the impetus for development of an extensive theory of stochastic processes.[1,2] The smaller the system, the greater will be the influence of fluctuations, given that their amplitude generally scales like the square root of the system size. Of particular interest is the analysis of noise- or fluctuation-induced transitions out of metastable states and between bistable states in optical, electrical, or chemical systems.[3] Studies of chemical reactions, which are of most relevance here, are generally based on mean-field (MF) type descriptions of the systems where detailed microscopic configurations are approximated by their average properties, typically ignoring spatial correlations.

For systems where the state is specified by discrete numbers of particles perhaps of various types, e.g., chemical reactions, adsorption–desorption processes, etc., it is natural to develop MF birth–death-type master equations (ME's) for the population dynamics.[1] Specifically, these equations describe the evolution of the probabilities for having various numbers of particles in the system. However, most common is analysis of MF Fokker–Planck equations (FPE's) which may be obtained after further approximation in the large-size limit of ME's with the aid of a truncated Kramers–Moyal expansion.[1] The latter FPE's are often reformulated as equivalent stochastic Langevin equations.

Of particular interest in this work is the role of fluctuations in catalytic surface reactions. There are several recent studies of the role of fluctuations in reactions on single-crystal surfaces using the MF approach.[4–7] Our focus in this paper is in the analysis of fluctuation-induced transitions in bistable catalytic surface reactions, specifically CO oxidation on nanoscale Pt field-emitter-tips (FET's).[8–11] Recent experiments on FET's, where fluctuations play a critical role due to the nanoscale system size, provide tremendous new possibilities for modeling of surface reactions and for comparison with stochastic theories including those going beyond MF treatments.[10,12–14]

For surface reactions, one generally expects significant spatial correlations (e.g., due to reactant islanding induced by adspecies interactions), and thus the MF description will be inadequate. Indeed, simple models for CO oxidation with limited CO mobility produce discontinuous transitions between reactive and inactive states,[15,16] reminiscent of first-order phase transitions in equilibrium systems (where a complicated nucleation theory rather than the MF theory is needed to describe the detailed dynamics of transitions between these states). However, the actual behavior of CO oxidation is rather different, although still complex: certainly there are nontrivial spatial correlations (e.g., in the oxygen adlayer due to strong NN repulsions and due to limited mobility) which cannot be described by MF treatments, but the rapid mobility of adsorbed CO ensures the existence of MF type bistability rather than equilibrium Ising-type discontinuous transitions.[17,18]

The latter observation has prompted development of "hybrid" models for CO oxidation which incorporate nontrivial spatial correlations in the oxygen adlayer using a lattice-gas treatment, but which also account for bistability induced by rapid CO mobility via a MF treatment of

[a]Electronic mail: dajiang@fi.ameslab.gov
[b]Also at Department of Mathematics, Iowa State University, Ames, Iowa 50011.

CO.[17–21] These type of hybrid atomistic models raise interesting new questions for the analysis of fluctuation-induced transitions in (small) finite systems. Despite the incorporation of nontrivial spatial correlations, is behavior analogous to traditional mean-field stochastic reaction models, or is it fundamentally different (e.g., as in equilibrium Ising systems)? If the former applies, to what extent can traditional MF-type concepts such as ''effective potentials'' be applied? Also, can accurate (but approximate) ME's or FPE's be developed for such hybrid models? In this paper, we focus on these issues for a specific hybrid model for CO oxidation, concluding that mean-field-type behavior does apply.

In Sec. II, we introduce the ''hybrid'' atomistic model for CO oxidation used in this study. We present results of kinetic Monte Carlo (KMC) simulations for the model and elucidate the nature of bistability in small systems in Sec. III. In Sec. IV, we focus on the system size dependence, and introduce the effective potential picture, which is useful in understanding of behavior of both population distributions in the steady state, and transitions between reactive and inactive steady states. In an Appendix, we contrast behavior of the hybrid model for that with reaction models with finite mobility, where the latter is more like that in conventional equilibrium systems. Behavior approaching a cusp bifurcation point in the model, denoting the termination of the bistable region, is discussed in Sec. V. To put our study into a broader perspective, in Sec. VI, we present an approximate treatment of our ''hybrid'' atomistic model by formulating it as a population model which can be treated by master equations and by Fokker–Planck equations. Discussion and concluding remarks are presented in Sec. VII.

II. "HYBRID" ATOMISTIC MODEL FOR CO OXIDATION

It has been established that under UHV conditions CO oxidation on noble metal single crystal surfaces is through a Langmuir–Hinshelwood mechanism. Below ''gas'' denotes gas phase, and ''ads'' adsorbed phase. A ''canonical'' lattice gas model has been developed for the study of this reaction on a square lattice of adsorption sites.[10,22] The model has the following features: (a) CO(gas) adsorbs onto single empty sites at rate p_{CO}, and CO(ads) desorbs with rate d_{CO}; CO(ads) also hops rapidly to nearby empty sites; (b) O_2(gas) adsorbs dissociatively at diagonal or second NN (2NN) pair of empty sites at rate[23] p_{O_2}, provided all six additional NN sites are not occupied by O(ads) (this so-called eight-site rule reflects very strong NN O–O repulsions); (c) adjacent CO(ads) and O(ads) pairs react at rate k.

This model is different from the classic Ziff–Gulari–Barshad (ZGB) model[15] for monomer–dimer reaction in two important aspects.

(i) A strong nearest-neighbor (NN) repulsion between O(ads) is assumed. This will introduce $c(2\times2)$ superlattice ordering of CO(ads)[24,25] often observed in experiments, and also prevent any O poisoning transition found in the ZGB model but not observed experimentally.

(ii) CO(ads) diffusion is very rapid.[26] This feature is crucial in order to produce the strong hysteresis and bistability observed in experiments.

One important limiting regime is to assume CO(ads) hops infinitely quickly to nearby empty sites, so CO(ads) is randomly distributed on sites not occupied by O(ads). Now one just needs to keep track of the coverage (or total number of) CO(ads) on the surface. This is the so-called ''hybrid'' atomistic model, since in this model, CO(ads) are described by a MF variable, while O(ads) are described by an atomistic lattice-gas model.

Studies of this model typically set $p_{\mathrm{CO}}+p_{\mathrm{O}_2}=1$. Analysis is performed on $L\times L$ site square lattices with periodic boundary conditions representing a single facet on a FET. Of course, on real FET's, the boundary conditions are more complex, e.g., due to possible enhanced reactivity at step edges, and coupling between facets via CO diffusion. The latter feature can introduce complex multistability near the (global) cusp bifurcation point.[27] However, experiments on Pt FET's shows that fluctuations on different facets retain local characteristics[10] when the system is away from the cusp point. Thus essential features of fluctuations on small facets can be captured by modeling an isolated system. The purpose of this paper is to reveal features in small systems that are not specific to any particular prescription of boundary conditions.

If N_J denotes the instantaneous number of adsorbed species of type $J=$CO or O, then $\theta_J=N_J/L^2$ denotes the corresponding instantaneous coverage. Below, we mainly consider $\langle\theta_J\rangle$ which denote the time-averaged mean steady-state coverages.

KMC studies[22,28] reveal bistability for an *infinite* system for $d_{\mathrm{CO}}<d_c(k)$: a stable reactive steady state (with high $\langle\theta_{\mathrm{O}}\rangle$ and low $\langle\theta_{\mathrm{CO}}\rangle$) coexists with a stable inactive or near-CO-poisoned steady state (with high $\langle\theta_{\mathrm{CO}}\rangle$ and low $\langle\theta_{\mathrm{O}}\rangle$) for a range of $p_{s^-}<p_{\mathrm{CO}}<p_{s^+}$. One has $p_{s^+}-p_{s^-}\to0$, so that bistability disappears as $d_{\mathrm{CO}}\to d_c^-$, a cusp bifurcation analogous to a thermodynamic critical point (with exponents in the MF universality class for the hybrid model[29]). These stable states are connected by an unstable state producing an S-shaped plot of steady state $\langle\theta_j\rangle$ versus p_{CO}, for $j=$CO or O. For this model d_c increases with k, such that $d_c(0+)=0$, $d_c(1)=0.0525$, and $d_c(\infty)=2/3$.

Thus, behavior is analogous to that of MF rate equations for CO oxidation reaction models of this type. This is not surprising since, as a result of infinite CO diffusivity, the CO coverage can be treated as a MF parameter. From a different perspective, the infinite CO diffusion length plays a similar role as infinite-range interactions in conventional equilibrium statistical models.

III. BEHAVIOR IN NANOSCALE SYSTEMS: FLUCTUATIONS, STEADY-STATE PROBABILITY DISTRIBUTIONS, AND BISTABILITY

Based on the general theory of finite-state Markov processes,[2] the reaction model in any *finite* system has a *unique* steady state for any parameter choice. Thus, the steady state $\langle\theta_J\rangle$ versus p_{CO} exhibits single-valued rather than S-shaped multivalued behavior.[2] Note that the steady state average $\langle\cdots\rangle$ must be determined from infinite observation times. Zhdanova[13] demonstrated explicitly this single-

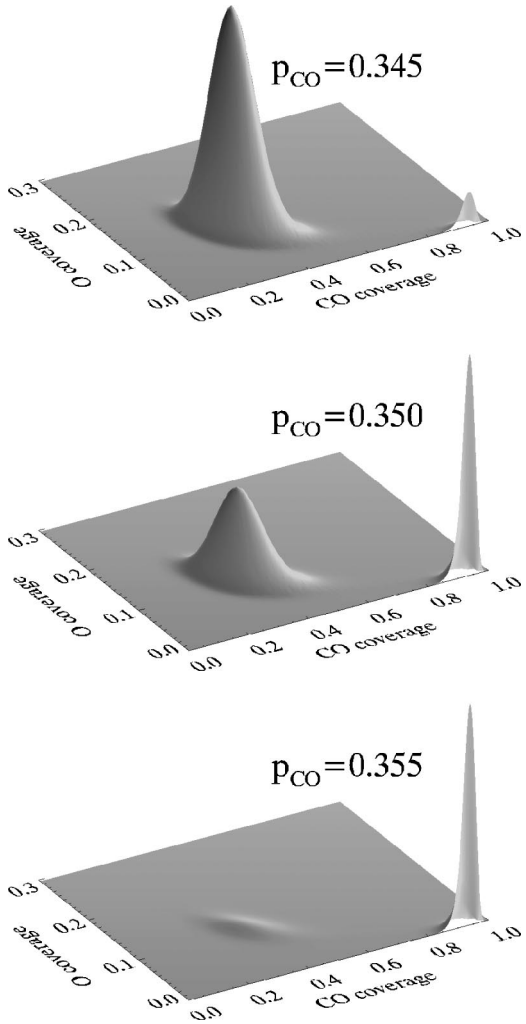

FIG. 1. $P(N_{CO},N_O)$ of the hybrid model with $L=16$, $k=1$, and $d_{CO}=0.02$.

valued monotonic behavior for very small systems by analysis of the exact master equations. However, it should be emphasized that this behavior follows immediately from the above general Markov theory for *all* finite size systems.

The above observations raise the question of what is the appropriate way to define bistability in finite systems. Zhdanova[13] argues that monotonic behavior of $\langle\theta_J\rangle$ (observed for very small systems) implies *no* bistability. However, as this monotonicity persists for all finite systems sizes, this is not the appropriate criterion. Another method is to search for ''hysteresis'' in θ_J as one scans p_{CO} back and forth.[14] However, this procedure also has shortcomings as some hysteresis always exists for finite scan rates, even in a monostable system (especially when close to a critical point). Also, large noise present in small ''bistable'' systems makes the analysis rather ambiguous, and the extent of hysteresis depends on the scan rate.

Instead, the natural quantity determining bistability is the normalized steady state probability distribution, $P(N_{CO},N_O)$, of finding N_{CO} adsorbed CO species on the surface, and N_O adsorbed O species (cf. Fig. 1). Then, one has

$$\langle\theta_J\rangle=\sum_{N_{CO},N_O}\theta_J P(N_{CO},N_O). \tag{1}$$

We *define* ''bistability'' to correspond to the occurrence of a ''bimodal'' distribution $P(N_{CO},N_O)$. In such cases, it is natural to introduce a deconvolution procedure,

$$P(N_{CO},N_O)=P^r(N_{CO},N_O)+P^i(N_{CO},N_O), \tag{2}$$

to separate the two peaks into components associated with reactive (r) and inactive (i) states. The population of these states are given by

$$P^i=\sum_{N_{CO},N_O}P^i(N_{CO},N_O) \tag{3}$$

and

$$P^r=\sum_{N_{CO},N_O}P^r(N_{CO},N_O). \tag{4}$$

''Equistability'' corresponds, e.g., to an equal population of these two states, i.e., $P^i=P^r$. One can define separate time-averaged mean coverages for these two states as

$$\langle\theta_J^r\rangle=\frac{1}{P^r}\sum_{N_{CO},N_O}\theta_J P^r(N_{CO},N_O) \tag{5}$$

and

$$\langle\theta_J^i\rangle=\frac{1}{P^i}\sum_{N_{CO},N_O}\theta_J P^i(N_{CO},N_O), \tag{6}$$

which will correspond closely to peak positions for larger systems. These coverages and populations (as well as equistability) depend somewhat on the deconvolution procedure, although all reasonable procedures will give the same result for well-separated peaks.

It is also useful to consider the reduced probability distribution,

$$P(N_{CO})=\sum_{N_O}P(N_{CO},N_O), \tag{7}$$

so one has $\langle\theta_{CO}\rangle=\Sigma_{N_{CO}}\theta_{CO}P(N_{CO})$. $P(N_{CO})$ will typically also be bimodal when $P(N_{CO},N_O)$ is bimodal. This follows noting that the peaks in $P(N_{CO},N_O)$ are more aligned with the direction of varying N_{CO} than that of varying N_O (cf. Fig. 1). Of course, deconvolution of $P(N_{CO})$ yields $P^r(N_{CO})$ and $P^i(N_{CO})$, as well as $\langle\theta_{CO}^r\rangle$ and $\langle\theta_{CO}^i\rangle$ somewhat modified from the above definitions at least for finite L.

It is appropriate to note that we can provide a simple interpretation of the unique steady states in this model for finite systems. Since such a system can always make fluctuation-induced transitions between the reactive and inactive ''states'' (given a sufficiently long time), the unique steady state is simply a weighted combination of these. The weights will shift continuously with increasing p_{CO} (favoring the inactive state), thus yielding a monotonic increase in $\langle\theta_{CO}\rangle$.

Figure 1 shows the behavior of $P(N_{CO},N_O)$ for $L=16$ with $k=1$ and $d_{CO}=0.02$ (cf., $d_c=0.0525$), for three different values of $p_{CO}=1-p_{O_2}$. $P(N_{CO},N_O)$ exhibits bimodal distribution in all three cases, but the relative weights of the

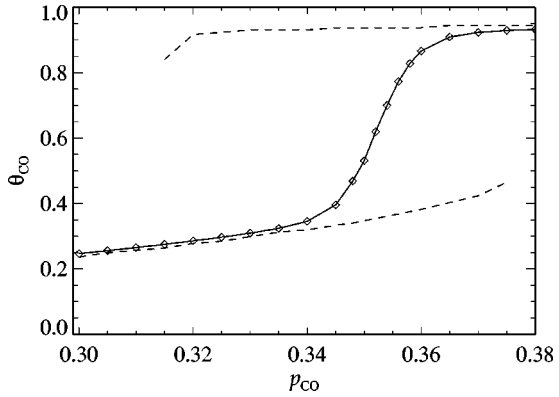

FIG. 2. $\langle \theta_{CO} \rangle$ (solid line and symbols), and the coverages corresponding to the two peaks in θ_{CO} distribution $P(N_{CO})$ (dashed lines) vs p_{CO} for the hybrid model. $L=12$, $k=1$, and $d_{CO}=0.02$.

two peaks shift with changing p_{CO}. Large p_{CO} values favor the inactive peak with high CO coverage and low O coverage.

It is natural to compare the behavior of steady state $\langle \theta_{CO} \rangle$, which vary monotonically with p_{CO}, with $\langle \theta_{CO}^r \rangle$ and $\langle \theta_{CO}^i \rangle$. The solid line in Fig. 2 plots $\langle \theta_{CO} \rangle$ versus p_{CO} for a system of $L=12$. Simulation results with 10^8 MC steps show that $P(N_{CO})$ has a double peak structure for p_{CO} between around 0.315 and 0.375. We also show the values of $\theta_{CO}=N_{CO}/L^2$ corresponding to the two peaks (and thus to $\langle \theta_{CO}^r \rangle$ and $\langle \theta_{CO}^i \rangle$) as the dashed lines in Fig. 2. Beyond this region of P_{CO}, the CO coverage has a single-peak distribution, and therefore the system is monostable. However, the exact boundaries between the monostable and bistable regions are difficult to determine, since it is hard to discern double-peaked structures when the two peaks are severely imbalanced.

Finally, we show in Fig. 3 a different representation of the probability distribution via a contour plot of the quantity $\phi_\Omega=\Omega^{-1}\ln[\Omega^2 P(N_{CO},N_O)]$, where $\Omega=L^2$, corresponding to an effective potential discussed in detail in Sec. IV.

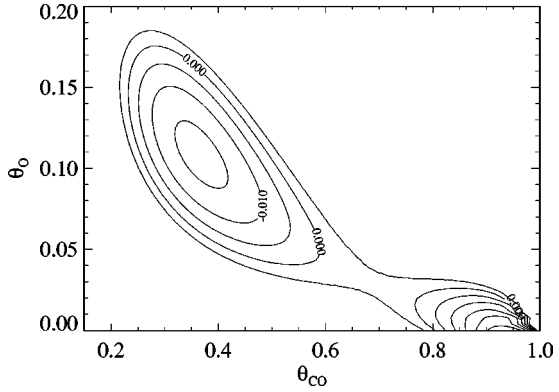

FIG. 3. Contour plot of $\phi_\Omega(\theta_{CO},\theta_O)$ for $L=16$, $p_{CO}=0.354$, $k=1$, and $d_{CO}=0.02$.

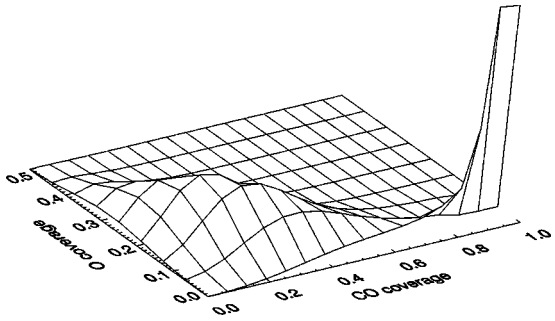

FIG. 4. $P(N_{CO},N_O)$ for $L=4$, $p_{CO}=0.32$, $k=1$, and $d_{CO}=0.02$.

IV. SIZE SCALING OF PROBABILITY DISTRIBUTIONS AND TRANSITION TIMES: TWO-WELL EFFECTIVE POTENTIALS

A. Steady state probability distribution

In this section, we determine the scaling behavior of $P(N_{CO},N_O)$ for varying L. First, it is appropriate to note that bistability (according to our definition) persists for extremely small sizes (contrasting the perception from other studies[13,14]). Figure 4 shows $P(N_{CO},N_O)$ for a system of 4×4. It has a bimodal distribution as in larger systems. We note that such bimodal distribution persists even to system of size 2×2.

Figure 5 shows $\langle \theta_{CO} \rangle$ versus p_{CO} for different system sizes. As in the case of equilibrium first-order phase transition, the transition is rounded for finite systems, and becomes sharper as L increases. Analysis below in terms of an effective potential can be used to quantify the nature of this sharpening, and the approach to a discontinuity, as $L\to\infty$. Note that this is under the condition that the observation time is first taken to be infinity. Otherwise, $\langle \theta_{CO} \rangle$ will display hysteresis if the observation time is comparable or less than the transition time between the two states (see Sec. IV B).

To compare probability distribution for systems of different sizes, it is convenient to define

$$\rho_\Omega(\theta_{CO},\theta_O)=\Omega^2 P(N_{CO},N_O), \tag{8}$$

and similarly,

$$\rho_\Omega(\theta_{CO})=\Omega P(N_{CO}), \tag{9}$$

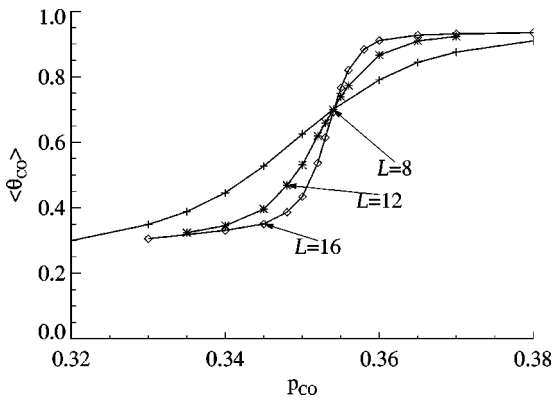

FIG. 5. $\langle \theta_{CO} \rangle$ vs p_{CO} for $L=8$, 12, and 16, with $k=1$ and $d_{CO}=0.02$.

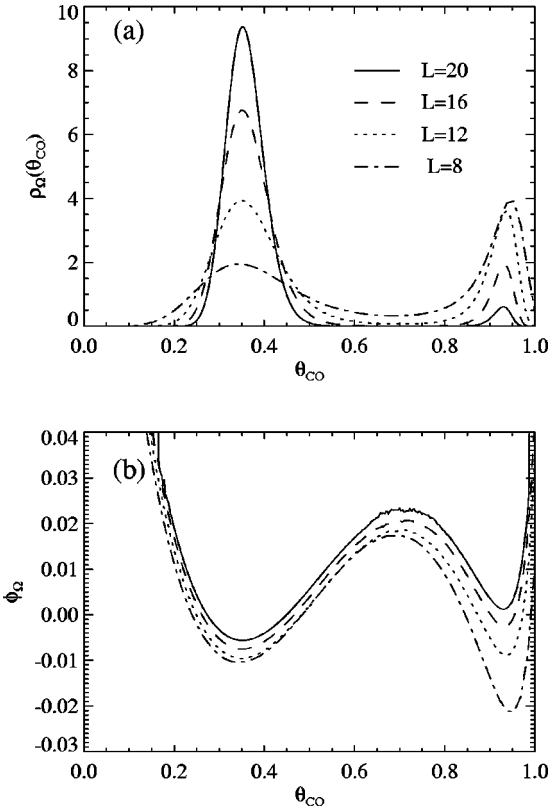

FIG. 6. (a) $\rho_\Omega(\theta_{CO})$ and (b) $\phi_\Omega(\theta_{CO})$ for systems of different sizes. $p_{CO}=0.35$, $k=1$, and $d_{CO}=0.02$.

where the factors of system size $\Omega=L^2$ are included so that the distributions are normalized under integration over continuous coverage variables. In Fig. 6(a) we compare $\rho_\Omega(\theta_{CO})$ for $L=8$ to 20, with $p_{CO}=0.35$, $d_{CO}=0.02$ and $k=1$. The parameters are chosen so that the system is in the bistable region.

For large systems, we assume that the probability distribution has the following form:

$$\rho_\Omega(\theta_{CO},\theta_O)\sim\exp[-\Omega\phi(\theta_{CO},\theta_O)]. \tag{10}$$

One interpretation of Eq. (10) is that ρ_Ω corresponds to the Boltzmann distribution for a potential field ϕ in the (θ_{CO},θ_O) space, with Ω corresponding to $(k_BT)^{-1}$ for thermodynamic systems. Hence, we call $\phi(\theta_{CO},\theta_O)$ the effective potential. It has a double-well structure in the bistable region. The probability distribution $\rho_\Omega(\theta_{CO})$ also has a similar potential form, $\rho_\Omega(\theta_{CO})\sim e^{-\Omega\phi(\theta_{CO})}$, where the local maxima and minima of $\phi(\theta_{CO})$ have the same limiting values in θ_{CO} as those of $\phi(\theta_{CO},\theta_O)$ as $\Omega\to\infty$. The existence of such effective potentials in nonequilibrium systems, which do not satisfy detailed balance, has been postulated in other contexts.[30]

In Fig. 6(b), we plot the quantity $\phi_\Omega(\theta_{CO})\equiv-\ln\rho_\Omega(\theta_{CO})/\Omega$ using results from Fig. 6(a). Finite size corrections are significant for systems of these sizes. Numerical analysis shows that (the shape of) ϕ_Ω converges as $\Omega\to\infty$ with corrections scale as $1/\Omega$.

As mentioned earlier, we can use the effective potential in Eq. (10) to quantify the sharpening of the transition as Ω increases. Denote $\Delta\phi=\phi(\theta^r_{CO})-\phi(\theta^i_{CO})$, then as $\Omega\to\infty$, one has that

$$\chi\equiv\frac{\partial\langle\theta_{CO}\rangle}{\partial p_{CO}}\approx\Omega\frac{(\theta^i_{CO}-\theta^r_{CO})\dfrac{\partial\Delta\phi}{\partial p_{CO}}}{(e^{-\Omega\Delta\phi/2}+e^{\Omega\Delta\phi/2})^2}. \tag{11}$$

For large Ω, χ reaches its maximal value, χ_{max}, near the equistability point where $\Delta\phi=0$. Assuming $\partial\Delta\phi/\partial p_{CO}\neq0$ is well-defined, then we have $\chi_{max}\sim\Omega$. Hence, the width of the region of p_{CO} where $\langle\theta_{CO}\rangle$ makes the transition between θ^r_{CO} and θ^i_{CO} scales as $1/\Omega$. This size scaling is similar to that found in equilibrium first-order phase transitions in finite systems.[31] Results shown in Fig. 5 are consistent with this scaling.

B. Transition between states

Any finite system can and will make transitions between the reactive and inactive states. It is clear that these transitions will be frequent if the fluctuations are sufficiently large that the steady state probability distribution is broad enough to have a significant value at the saddle point. Otherwise transitions will be infrequent. Of particular interest are the residence times, T^i (T^r), for the system to stay in the inactive (reactive) state before it makes a transition to the reactive (inactive) state. As a consequence of the fluctuation-induced nature of the transition, T^i and T^r are random variables. Note that they are related to the relative populations of the two states by $\langle T^i\rangle/\langle T^r\rangle\approx P^i/P^r$.

The potential picture in Eq. (10) can also give prediction to the effects of system sizes on the transition time. One can view the transition between the two states as noise-induced diffusion over the barriers of the effective potential ϕ. For large Ω (low noise or low effective temperature), the escape times from the two states are approximately[1–3,32]

$$\langle T^r\rangle\sim e^{\Omega\Delta\phi^r} \tag{12}$$

and

$$\langle T^i\rangle\sim e^{\Omega\Delta\phi^i}, \tag{13}$$

where $\Delta\phi^r$ and $\Delta\phi^i$ are the differences in the values of $\phi(\theta_{CO},\theta_O)$ between the saddle point and the two local minima corresponding to the reactive state and inactive state, respectively. Observing that the equipotential line for $\phi(\theta_{CO},\theta_O)$ at the saddle point is mostly aligned with the θ_{CO} direction, the one-variable effective potential $\phi(\theta_{CO})$ should give a good estimate of the potential barriers (in the regime of large L).

It is rather difficult to acquire good statistics directly for the transition times. This is because there is no clear distinction between what amounts to transition between states and very large fluctuations away from one of the state. In practice, it is more convenient to consider the time correlation function:

$$C(t)=\langle(\theta(t)-\langle\theta\rangle)(\theta(0)-\langle\theta\rangle)\rangle. \tag{14}$$

Assuming the transitions between the two steady states are independent Poisson processes with average transition time $\langle T^i\rangle$ and $\langle T^r\rangle$, respectively, analysis shows[33] that the correlation function has the form

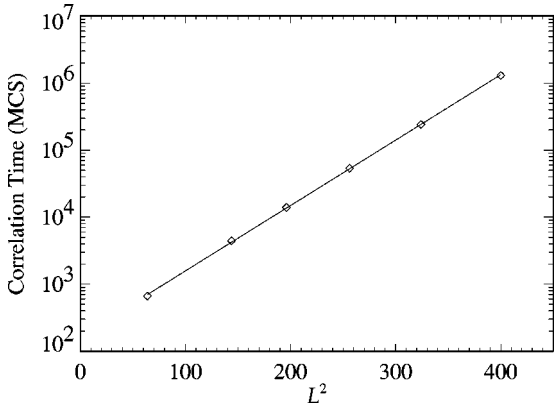

FIG. 7. Correlation time from $\theta_{CO}(t)$ for systems of sizes $L=8$ to 20. Other parameters are $p_{CO}=0.354$, $k=1$, and $d_{CO}=0.02$. The solid line is a fit to $\exp(-L^2\delta\phi)$ with $\delta\phi=0.0225(2)$.

$$C(t)=(\langle\theta^r\rangle-\langle\theta^i\rangle)^2\frac{\langle T^r\rangle\langle T^i\rangle}{\langle T^r+T^i\rangle^2}e^{-t/\tau}, \tag{15}$$

where the correlation time τ satisfies

$$\frac{1}{\tau}=\frac{1}{\langle T^r\rangle}+\frac{1}{\langle T^i\rangle}. \tag{16}$$

Therefore near the equistability point where $\Delta\phi^r=\Delta\phi^i$ and $\langle T^i\rangle=\langle T^r\rangle$, the correlation time has the following exponential form:

$$\tau\sim e^{\Omega\Delta\phi^r}=e^{\Omega\Delta\phi^i}. \tag{17}$$

Figure 7 plots the correlation time for systems of different sizes near the equistability point with $p_{CO}=0.354$, $k=1$, and $d_{CO}=0.02$. As predicted by Eqs. (12) and (13), it has an exponential dependence on $\Omega=L^2$. By fitting the logarithm of the correlation time versus Ω by a straight line, we obtain $\delta\phi=0.0225(2)$. By analyzing probability distribution $\rho(\theta_{CO})$ directly, we obtain $\delta\phi=0.0219(5)$, in good agreement with the result from the dynamical study.

V. BEHAVIOR APPROACHING A CUSP BIFURCATION POINT

We have noted above that for infinite systems that the region of bistability in the hybrid reaction model becomes smaller with increasing CO desorption rate, d_{CO}, and eventually disappears at some critical value, d_c.[22] This transition corresponds to a cusp bifurcation, so that the region of bistability in p_{CO} decrease linearly as d_{CO} approaches d_c. The behavior at the *equistability* point is phenomenologically described by a reduced effective potential of the Landau form

$$\phi(\theta_{CO})=-\tfrac{1}{2}A\delta\theta_{CO}^2+\tfrac{1}{4}B\delta\theta_{CO}^4. \tag{18}$$

Here, we set $\delta\theta_{CO}=\theta_{CO}-\theta_{CO}^s$, and assume that $A\sim a(d_c-d_{CO})$, with $a>0$, and that $B>0$ is weakly dependent on d_{CO}. For $A>0$, Eq. (18) has a local maximum at θ_{CO}^s and two local minima at $\theta_{CO}^s\pm\sqrt{A/B}$, which correspond to the steady state coverage for the reactive state θ_{CO}^r and inactive state θ_{CO}^i, respectively. Thus one has for $d_{CO}<d_c$, $\theta_{CO}^i-\theta_{CO}^r=2\sqrt{A/B}=2\sqrt{a/B}(d_c-d_{CO})^{1/2}$. More importantly, the potential barrier between the reactive and inactive states is given by

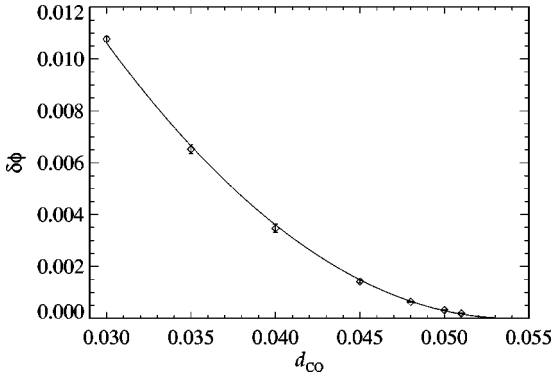

FIG. 8. Barrier height of the effective potential near the equistability point for $L=16$. The solid line is a fit to $a(d_c-d_{CO})^2$, where $d_c=0.054$.

$$\delta\phi=\phi(\theta_{CO}^s)-\phi(\theta_{CO}^r)$$
$$=\phi(\theta_{CO}^s)-\phi(\theta_{CO}^i)=A^2/(4B)\sim(d_c-d_{CO})^2. \tag{19}$$

Figure 8 shows the potential barrier between the two local minima of $\phi(\theta_{CO})$ near the equistability pressure for different d_{CO} values. The system size is $L=16$. The barrier vanishes quadratically as d_{CO} approach the critical point, consistent with the above MF prediction of the Landau theory.

VI. EXACT VERSUS APPROXIMATE TREATMENTS

For an *infinite* system, the hybrid model is described by the rate equations

$$\frac{d}{dt}\theta_{CO}=w_{COads}-w_{COdes}-w_{react} \tag{20}$$

and

$$\frac{d}{dt}\theta_{O}=2w_{O_2ads}-w_{react}, \tag{21}$$

with the exact relations

$$w_{COads}=p_{CO}(1-\theta_{CO}-\theta_O), \tag{22}$$

$$w_{COdes}=d_{CO}\theta_{CO}, \tag{23}$$

and

$$w_{react}=4k\theta_O\theta_{CO}^{loc}, \tag{24}$$

where $\theta_{CO}^{loc}=\theta_{CO}/(1-\theta_O)$ is the local coverage of CO on non-O-covered sites. The only term which cannot be simply described in terms of coverages is the O_2 adsorption rate, which can be written as $w_{O_2ads}=p_{O_2}s_{O_2ads}$, where s_{O_2ads} is the normalized sticking probability for oxygen, i.e., the probability of finding two next NN empty sites with all six NN not occupied by oxygen. One can precisely determine the behavior of this quantity via simulations, or one can introduce analytic approximations. In particular, we mention the Kirkwood-type ''pair approximation'' wherein[22]

$$s_{O_2ads}(\theta_{CO},\theta_O)=\frac{(1-\theta_{CO}-\theta_O)^2(1-2\theta_O)^8}{(1-\theta_O)^{10}}. \quad (25)$$

In this section, we focus on different treatments of the hybrid model for *finite* systems.

A. "Exact" simulation study

To precisely analyze an atomistic dynamical model, one usually needs the help of computer simulations, particularly kinetic Monte Carlo (KMC) simulations. We have used extensively the KMC method in the text and focus on simulation results for the population of CO and O, but simulations can probe all other aspects of behavior of the model as well. One example is the detailed distribution of oxygen on the surface: due to strong repulsion between NN oxygen atoms, the oxygen adlayer undergoes an ordering transition from short-range order at low θ_O to $c(2\times2)$ long-range order at high θ_O. The transition belongs to the (non-MF) Ising universality class, even though the description of CO is MF in the "hybrid" model.[24,25]

One disadvantage of computer simulations is that to some extent they operate like a "black box." One can only gain limited insight into the underlying causes of observed behavior. Therefore, it is useful to consider other more analytic (but approximate) approaches to the problem, such as the master equations and Fokker–Planck equations discussed below.

B. Master equation

One approach to analyzing the atomistic model (and more general chemical processes) is to reformulate it as a population model for a "birth–death" process. This type of model has been instrumental in studying stochastic processes.[1] Recently it has been applied to the CO oxidation problem.[7,12]

The population model is essentially a MF approximation of the atomistic model. Instead of microscopic configurations and processes of adsorbates, one only tracks the total numbers (or equivalently coverages) of adsorbates of different species and their increment and decrement. The population model and its master equations treatment are described in more detail in Ref. 12. Here we recap some essential ingredients. For the CO oxidation model described in Sec. II, there are four processes that can change the populations of CO(ads) and O(ads):

(i) CO adsorption: $(N_{CO},N_O)\rightarrow(N_{CO}+1,N_O)$, with rate W_{COads}.
(ii) CO desorption: $(N_{CO},N_O)\rightarrow(N_{CO}-1,N_O)$, with rate W_{COdes}.
(iii) O_2 adsorption: $(N_{CO},N_O)\rightarrow(N_{CO},N_O+2)$, with rate W_{O_2ads}.
(iv) CO+O reaction: $(N_{CO},N_O)\rightarrow(N_{CO}-1,N_O-1)$, with rate W_{react}.

For convenience, let us denote the populations by a vector $\mathbf{N}=(N_{CO},N_O)$, and its change for each process α by a vector $\mathbf{M}_\alpha$. For example, for the first process CO adsorption, populations will change from $\mathbf{N}$ to $\mathbf{N}+\mathbf{M}_1$, where $\mathbf{M}_1=(1,0)$. Evolution of the probability distribution $P(N_{CO},N_O)$ is governed by the *master equations* (ME):

$$\partial_t P(\mathbf{N})=\sum_{\alpha=1}^{4}\left[W_\alpha(\mathbf{N}-\mathbf{M}_\alpha)P(\mathbf{N}-\mathbf{M}_\alpha)-W_\alpha(\mathbf{N})P(\mathbf{N})\right]. \quad (26)$$

In Ref. 12, we have given the explicit form of the ME using pair approximations. Here suffice it to note that W_α can be approximately given by Ωw_α in Eqs. (22)–(25). Numerical solutions of Eq. (26) for the steady states produce bimodal distributions in $P(\mathbf{N})$ in bistable regions, recovering semiquantitatively results from simulations.

C. Fokker–Planck equation

It is particularly instructive to examine the form of the ME in the limit of large systems, where we introduce continuous variables $\theta_{CO}=N_{CO}/\Omega$ and $\theta_O=N_O/\Omega$. Truncating the Kramers–Moyal expansion[1] of the ME to second order gives

$$\partial_t\rho=\left[-\sum_i\frac{\partial}{\partial\theta_i}D_i^{(1)}+\sum_{i,j}\frac{\partial^2}{\partial\theta_i\partial\theta_j}D_{ij}^{(2)}\right]\rho, \quad (27)$$

where $i,j=1$ or 2 denotes CO and O, respectively, and

$$D^{(1)}=\begin{pmatrix} w_{COads}-w_{COdes}-w_{react} \\ 2w_{O_2ads}-w_{react}\end{pmatrix}, \quad (28)$$

$$D^{(2)}=\frac{1}{2\Omega}\begin{pmatrix} w_{COads}+w_{COdes}+w_{react} & w_{react} \\ w_{react} & 4w_{O_2ads}+w_{react}\end{pmatrix}. \quad (29)$$

Equation (27) is a Fokker–Planck equation (FPE). The first term is the drift term, which describes the deterministic evolution of the population model. The second term is the diffusion term, which describes the fluctuations. By defining a probability current[32]

$$S_i=D_i^{(1)}\rho-\sum_j\frac{\partial}{\partial\theta_j}D_{ij}^{(2)}\rho, \quad (30)$$

Eq. (27) has the form of the continuity equation

$$\partial_t\rho+\nabla\cdot\mathbf{S}=0. \quad (31)$$

The stationary solution then satisfies $\nabla\cdot\mathbf{S}=0$. It is expected that under some conditions, the stationary solution of Eq. (27) has an asymptotic form in the weak-noise (i.e., large Ω) limit

$$\rho(\theta_{CO},\theta_O)\sim\exp[-\Omega\phi(\theta_{CO},\theta_O)]. \quad (32)$$

The nonequilibrium potential ϕ satisfies[34]

$$\sum_i D_i^{(1)}\frac{\partial\phi}{\partial\theta_i}+\sum_{i,j}\frac{1}{2}Q_{ij}\frac{\partial\phi}{\partial\theta_i}\frac{\partial\phi}{\partial\theta_j}=0, \quad (33)$$

where $Q_{ij}=(2\Omega)D_{ij}^{(2)}$.

In the limit of $\Omega\rightarrow\infty$, Eq. (27) reduces to the deterministic rate equations:

$$\partial\theta_i/\partial t=D_i^{(1)}. \quad (34)$$

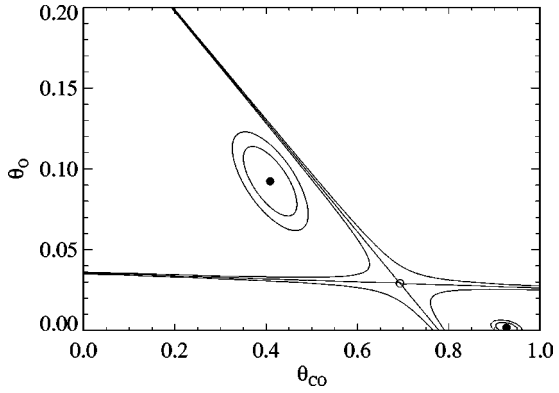

FIG. 9. Contour plot of ϕ near the three fixed points derived from the Fokker–Planck equation (27). Parameters used are $p_{CO}=0.35$, $d_{CO}=0.02$, and $k=1$. Solid lines are equipotential lines, with consecutive separation of 0.002. Filled circles are the two stable fixed points and the empty circle is the unstable fixed point.

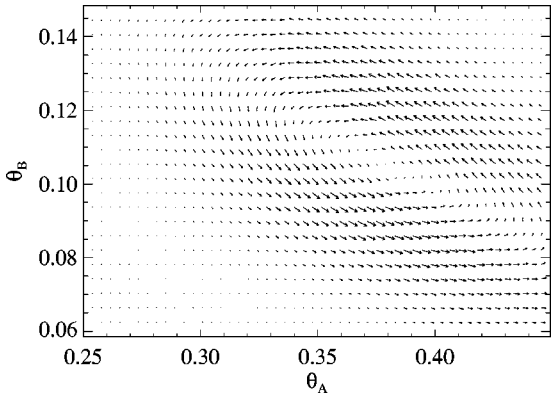

FIG. 10. Flow of probability current in the stationary state for $L=16$, $p_{CO}=0.354$, $k=1$, and $d_{CO}=0.02$.

Depending on the parameters, Eq. (34) has either one or three fixed points. In the latter case, two of the fixed points will be stable, and one of them will be unstable. Let A_{ij} be the Jacobian matrix for the rate equations (34) evaluated at a fixed point, so that $D_i^{(1)} \approx \Sigma_j A_{ij}(\theta_j - \theta_j^*)$. By assuming ϕ has a quadratic form

$$\phi \approx \sum_{i,j} \tfrac{1}{2}(\sigma^{-1})_{ij}(\theta_i - \theta_i^*)(\theta_j - \theta_j^*), \quad \sigma_{ij} = \sigma_{ji} \tag{35}$$

near a fixed point $(\theta_{CO}^*, \theta_O^*)$ of the deterministic rate equations, Eq. (33) gives[34]

$$(A\sigma)_{ij} + (A\sigma)_{ij}^T = -Q_{ij}, \tag{36}$$

from which one can solve for σ_{ij}. Figure 9 shows local potential near the three fixed points. It has two wells around the two stable fixed points, and a saddle point at the unstable fixed point.

To find the barrier height between the potential wells and the saddle point, one must solve for the complete nonlinear equation (33), with appropriate boundary conditions. This is a very difficult numerical problem. As a crude approximation, one can piece together local expansions about the fixed points to obtain reasonable estimate of barrier heights.

Note that the solution of the FPE obtained from truncating Kramers–Moyal expansions is only an approximation of the original ME, even in the large Ω limit. Specifically, for a bistable system, the barrier heights of $\phi(\theta_{CO}, \theta_O)$ obtained from Eq. (27) will be different from the one obtained from the ME (26). See Hanggi *et al.*[35] for the case of one-variable ME's and FPE's.

D. Violation of detailed balance and probability current

We have shown in preceding sections that bistable behavior in our surface reaction model is very much analogous to that in a Landau-type MF treatment of first-order phase transitions in equilibrium systems. However, unlike in equilibrium systems, detailed balance is not satisfied in the reaction model. For the atomistic model or the corresponding population model, this is rather transparent, since both O_2 adsorption and CO-O reaction are irreversible. Below we discuss some consequences of violation of detailed balance.

In Eq. (30) we define the probability current for the FPE, and the stationary solution corresponds to the condition $\nabla \cdot \mathbf{S} = 0$. For multivariable FPE's, the stationary probability current generally does not vanish, unless detailed balance is satisfied. Although $\mathbf{S}$ is most readily defined for the FPE's, the discrete version of the probability current can also be constructed for the atomistic model (and also for the master equations).

To measure the probability current for the atomistic model using Monte Carlo simulations, we record as a histogram the frequency of each process *starting from* the configuration with N_{CO} CO(ads) and N_O O(ads). We then decompose the microscopic current associated with the four microscopic processes along the two directions of N_{CO} and N_O:

$$S_{CO} = S_{COads} - S_{COdes} - S_{react} \tag{37}$$

and

$$S_O = 2S_{O_2ads} - S_{react}. \tag{38}$$

Figure 10 shows the probability current thus defined from Monte Carlo simulations of the ''hybrid'' atomistic model. It shows a counter-clockwise nonvanishing current.

VII. CONCLUSIONS

Our analysis demonstrates the existence of bistability in the hybrid reaction model for CO oxidation in finite systems. We provide numerical evidence to indicate the existence of an effective potential characterizing this behavior. This potential is determined by ''exact'' KMC simulation analysis, but reasonable estimate available from approximate master (or population) equations, and from Fokker–Planck equations which are obtained from further approximation of the master equations.

Precise KMC analysis of the ''hybrid'' atomistic model validates various qualitative predictions of the master equations and Fokker–Planck equations, which constitute a mean-field treatment of stochastic systems. This is a consequence of rapid CO diffusion which plays an important role making the system ''well-stirred.'' This is a realistic picture for chemical systems if the size of the system is smaller than the diffusion length of one of the reacting species involved in

the transitions. Therefore, diffusion plays a role similar to long-range interactions in equilibrium statistical mechanical systems. On the other hand, if the system is much larger than a certain function of the relevant diffusion lengths, a picture more analogous to equilibrium systems with short-ranged interactions is more appropriate. Specifically, the barrier of the effective potential in the bistable regime will decrease as the system size increases, and the transition time scales as e^{cL} rather than e^{cL^2}. See the Appendix.

ACKNOWLEDGMENTS

This work was supported by the Division of Chemical Sciences, USDOE–BES. It was performed at Ames Laboratory, which is operated for the USDOE by Iowa State University under Contract No. W-7405-Eng-82. The authors also acknowledge valuable discussions and collaborations with Professor Ronald Imbihl and his co-workers.

APPENDIX: FINITE CO-DIFFUSION MODEL

In the main body of this paper, we have exclusively studied a ''hybrid'' reaction model where the CO diffusion rate is assumed to be infinite. The results are relevant to most catalytic CO oxidation experiments where CO diffusion is indeed much faster than all other relevant processes. In this Appendix, we briefly discuss a complementary model where the CO diffusion rate is finite. In this model, each individual CO(ads) is tracked and it can hop to one of its (four) NN sites with hopping rate h_{CO}, provided that the final site is unoccupied.

Compared with the ''hybrid'' model, finite CO diffusion allows a system to become spatially inhomogeneous, i.e., it allows for the coexistence of regions of reactive and inactive states. Mean-field behavior breaks down when there are large inhomogeneities in the system. Specifically, the size scaling behavior identified for the ''hybrid'' model of both the probability distribution [Eq. (10)] and the transition times [Eqs. (12) and (13)] does not hold for the finite h_{CO} model. Here, it is appropriate to comment on the analogy between bistability in the reaction system and an equilibrium first-order transition. The effective potential $\phi_\Omega(\theta_{\mathrm{CO}},\theta_{\mathrm{O}})$ in Eq. (10) is reminiscent of the coarse-grained free energy density divided by k_BT for an equilibrium system. For equilibrium systems with finite-ranged interactions, e.g., the Ising model, the (scaled) potential barrier between the double wells will flatten, and the potential between the two phases becomes a straight line segment, as $L\to\infty$, approaching the thermodynamical free energy. This requires spatial inhomogeneity. However, for the ''hybrid'' model, the lack of spatial inhomogeneity due to the infinitely fast CO diffusion ensures that the double-well structure will persist in the limit of $L\to\infty$. This is similar to the Ising model with infinite-range interactions.

The decrease in the potential barrier for the finite CO diffusion model means that the transition times between states have a weaker size dependence than for the ''hybrid'' model or MF behavior. Figure 11 is a log-linear plot of the correlation time versus L, the linear dimension of the system. It shows that the system size dependence of the relaxation time τ can be approximately given by

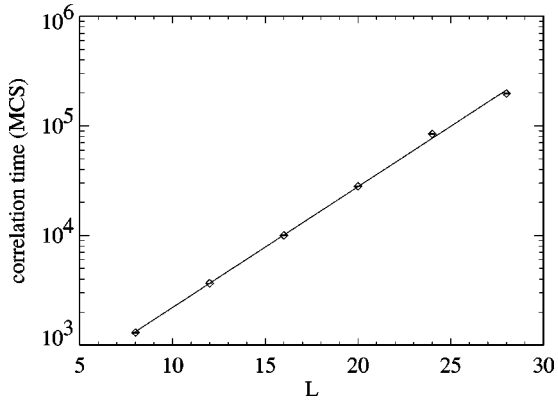

FIG. 11. Correlation time of $\theta_{\mathrm{CO}}(t)$ vs system sizes for the reaction model with a finite CO diffusion rate. Parameters used are $k=1$, $h_{\mathrm{CO}}=2$, $p_{\mathrm{CO}}=0.3376$ (close to the first-order transition, where $p_{\mathrm{CO}}\to 0.339$ for $L\to\infty$), and $d_{\mathrm{CO}}=0.02$ (below the critical value of 0.025). The solid line is a fit to $\exp(-L\phi_{\mathrm{int}})$.

$$\tau\sim e^{cL}. \tag{A1}$$

One can understand this behavior by drawing an analogy to equilibrium first-order transitions. To go from one state to the other, the system can first nucleate a domain of the other state. Then the domain can grow (relatively quickly) and spread over the whole system. The typical length of the domain boundary is L, thus the activation barrier of nucleation is $L\phi_{\mathrm{int}}$, where ϕ_{int} is the interfacial tension. For the reaction system, we can identify ϕ_{int} as the effective interfacial tension of the ''reaction front'' between the reactive and inactive states.

[1] C. W. Gardiner, *Handbook of Stochastic Methods for Physics, Chemistry and the Natural Sciences*, Springer Series in Synergetics (Springer-Verlag, Berlin, 1983).
[2] N. G. van Kampen, *Stochastic Processes in Physics and Chemistry* (North-Holland, Amsterdam, 1992).
[3] H. Malchow and L. Schimansky-Geier, *Noise and Diffusion in Bistable Nonequilibrium Systems*, Teubner Texte zur Physik (Teubner Verlag, Leipzig, 1986).
[4] M. Hildebrand and A. S. Mikhailov, J. Phys. Chem. **100**, 19089 (1996).
[5] M. Hildebrand, Chaos **12**, 144 (2002).
[6] R. Kapral and X.-G. Wu, J. Phys. Chem. **100**, 18976 (1996).
[7] C. Reichert, J. Starke, and M. Eiswirth, J. Chem. Phys. **115**, 4829 (2001).
[8] Y. Suchorski, J. Beben, and R. Imbihl, Prog. Surf. Sci. **59**, 343 (1998).
[9] Y. Suchorski, J. Beben, and R. Imbihl, Surf. Sci. **405**, L477 (1998).
[10] Y. Suchorski, J. Beben, E. W. James, J. W. Evans, and R. Imbihl, Phys. Rev. Lett. **82**, 1907 (1999).
[11] Y. Suchorski, J. Beben, and R. Imbihl, Surf. Sci. **454–456**, 331 (2000).
[12] Y. Suchorski, J. Beben, R. Imbihl, E. W. James, D.-J. Liu, and J. W. Evans, Phys. Rev. B **63**, 165417 (2001).
[13] A. V. Zhdanova, Phys. Rev. B **63**, 153410 (2001).
[14] V. P. Zhdanov and B. Kasemo, Surf. Sci. **496**, 251 (2002).
[15] R. M. Ziff, E. Gulari, and Y. Barshad, Phys. Rev. Lett. **56**, 2553 (1986).
[16] J. W. Evans and T. R. Ray, Phys. Rev. E **50**, 4302 (1994).
[17] M. Tammaro, M. Sabella, and J. W. Evans, J. Chem. Phys. **103**, 10277 (1995).
[18] J. W. Evans, D.-J. Liu, and M. Tammaro, Chaos **12**, 131 (2002).
[19] M. Silverberg, A. Ben-Shaul, and F. Rebentrost, J. Chem. Phys. **83**, 6501 (1985).
[20] M. Silverberg, and A. Ben-Shaul, J. Chem. Phys. **87**, 3178 (1987).
[21] M. Silverberg and A. Ben-Shaul, Chem. Phys. Lett. **134**, 491 (1987).
[22] E. W. James, C. Song, and J. W. Evans, J. Chem. Phys. **111**, 6579 (1999).
[23] This means that the impingement rate for O_2 (gas) per 2NN pair of sites is $p_{O_2}/2$ since there are two pairs per lattice site.

[24] D.-J. Liu and J. W. Evans, Phys. Rev. Lett. **84**, 955 (2000).
[25] D.-J. Liu and J. W. Evans, Phys. Rev. B **62**, 2134 (2000).
[26] J. V. Barth, Surf. Sci. Rep. **40**, 75 (2000).
[27] N. Pavlenko, J. W. Evans, D.-J. Liu, and R. Imbihl, Phys. Rev. E **65**, 016121 (2002).
[28] V. P. Zhdanov and B. Kasemo, Surf. Sci. **412/413**, 527 (1998).
[29] N. Pavlenko *et al.* (unpublished); D.-J. Liu *et al.* (unpublished).
[30] R. Kubo, K. Matsuo, and K. Kitahara, J. Stat. Phys. **9**, 51 (1973).
[31] M. E. Fisher and A. N. Berker, Phys. Rev. B **26**, 2507 (1982).
[32] H. Risken, *The Fokker-Planck Equation: Methods of Solution and Applications*, 2nd ed. Springer Series in Synergetics (Springer-Verlag, Berlin, 1989).
[33] R. L. Stratonovich, *Topics in the Theory of Random Noise* (Gordon and Breach, New York, 1963), Vol. 1, revised English edition, translated from the Russian by Richard A. Silverman.
[34] R. Graham, in *Stochastic Nonlinear Systems in Physics, Chemistry, and Biology*, edited by L. Arnold and R. Lefever (Springer, Berlin, 1981), p. 202.
[35] P. Hanggi, H. Grabert, P. Talkner, and H. Thomas, Phys. Rev. A **29**, 371 (1984).